Novel Double-Turn Loop Probe for Intravascular MRI

M. Mohammad-Zadeh,[1] H. Soltanian-Zadeh,[2,3] M. Shah-Abadi,[3] A.Tavakkoli[4]

[1]Department of Physics, Amir-Kabir University of Technology, Tehran, Iran
[2]Department of Radiology, Henry Ford Health System, Detroit, Michigan, USA
[3]Department of Electrical and Computer Engineering, University of Tehran, Tehran, Iran
[4]Department of Electrical Engineering, Amir-Kabir University of Technology, Tehran, Iran

Abstract— Key challenges for design of intravascular loop probes are minimization of the cross sectional and length while increasing signal-to-noise ratio (SNR). Although NPO grade captors under 1mm dimensions are now available, the impedance matching network components still constrain tunability. In this study, a new loop probe is proposed for intravascular magnetic resonance imaging (MRI) at 1.5 Tesla. The new design is based on a two-turn loop, separated by a gap, which can be placed over a perfused inflatable balloon structure. The length and impedance of the probe are 1.1cm and 23.5OHM (bare case), respectively. The SNR of the new probe is greater than the conventional loop probe. To evaluate the performance of the probe, a series of SNR, length, and impedance comparisons with the conventional loop probes are carried out.

Keywords: **Magnetic Resonance Imaging (MRI), loop antenna, intravascular probe.**

I. INTRODUCTION

Magnetic Resonance Imaging (MRI) loop probes, customized for specific applications, can provide significant improvements for the image signal-to-noise (SNR). In turn, this can be used for increased resolution. Loop probes have two limitations. Firstly, their tuning and matching circuits must be placed close to them inside the vessel. Secondly, their SNR is inversely proportional to the square of the distance from the probe [1,2,3]. We have proposed a new dual-turn loop probe to alleviate these limitations. In this paper, an analysis is presented for a bare and insulated open-ended loop probe inside a finite homogeneous medium. In addition, the advantages of the new probe to the conventional loop antennas are discussed from the viewpoint of SNR, size, and input impedance.

II. METHODOLOGY

A fidelity measure that is independent of the imaging parameters and the signal processing system is needed to compare and evaluate MRI probes. Such a meaure is intrinsic SNR, defined for a given sample-probe combination as the MR signal voltage received from a 1-cm cube of the sample divided by the root-mean-squre (RMS) of the noise voltage received per square-root of the bandwidth in Hertz [4,5]. Starting from the reciprocity principle [6], one obtains the intrinsic SNR as:

$$\psi_I = \frac{\sqrt{2}\omega\mu M_0 H_+}{\sqrt{4k_B TR}} \qquad (1)$$

where ω is the Larmor frequency, μ is the magnetic permeability of the sample, M_0 is the total transverse nuclear magnetic moment in a 1 ml sample, H_+ is the magnitude of the right-hand circularly polarized component of the magnetic field generated by the probe with unit input current, k_B is the Boltzmann constant, T is the sample temperature, and R is the real part of the probe's input impedance. In Eq. (1), H_+ and R are the only parameters of the probe that can be manipulated to improve the SNR of the probe. In other words, to evaluate the intrinsic SNR of a new probe, the magnitude of its magnetic field and its input impedance must be determined for a unit current applied to the probe input.

III. PROPOSED PROBE AND ITS ANALYSIS

Figure 1 depicts the proposed new loop probe. The radius of the wires used in the construction of the probe is 0.1 mm. The width of the loop is 4 mm. The wires are assumed to be covered by an insulating layer of ε_r= 3.3. The thickness of the insulating layer is a variable in the following discussions. In the special case of the bare wires, this thickness is set to zero. The surrounding medium of the loop is considered to be infinite with a relative permittivity of ε_r= 80 and a conductance of σ = 0.8 S/m. The working frequency of the probe is assumed to be 64 MHz which is the operating frequency of 1.5 Tesla MRI systems.

To evaluate H_+ and R for the proposed loop, we used a finite element method. As a result of this analysis, the current on the antenna conductors was determined. This was used to calculate the magnetic field and the input impedance of the loop. To this end, commercially available finite-element software was linked with MATLAB to allow the parameter sweep.

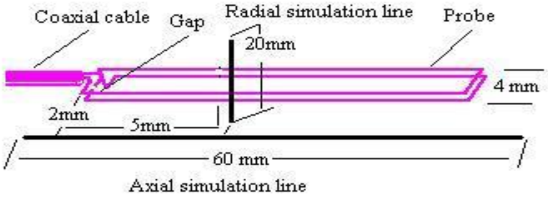

Fig. 1. The proposed new loop probe.

IV. *RESULTS*

A. *Effect of insulation on the resonance length and real part of the input impedance*

Figure 2.a shows that by increasing insulation thickness, the resonance length of the proposed probe increases while *R* decreases. The bare probe resonance length is 1.1 cm, which is nearly doubled to a value of 2.2 cm for 0.002 mm of insulation. For the conventional loop probe, there is no resonance length for the bare case and the resonance length starts above 10 cm for 0.002 mm of insulation and increses by increasing insulation thickness excessively. Figure 2.b shows that the impedance of the bare new loop is 23.5 OHM and with 0.1 mm of insulation, *R* drops by 80% compared to the bare case. Figure 2-c shows the real and imaginary parts of the impedance of the conventional loop probe increase with the insulation thickness. In addition, we observe that the real part of the impedance is very low (e.g., 0.7 OHM for the bare case) and the imaginary part is very large (e.g., 130 OHM for 0.1 mm insulation thickness) for any insulation thickness. Therefore, the use of matching and tuning circuits is necessary for the best signal transmission to the MRI system.

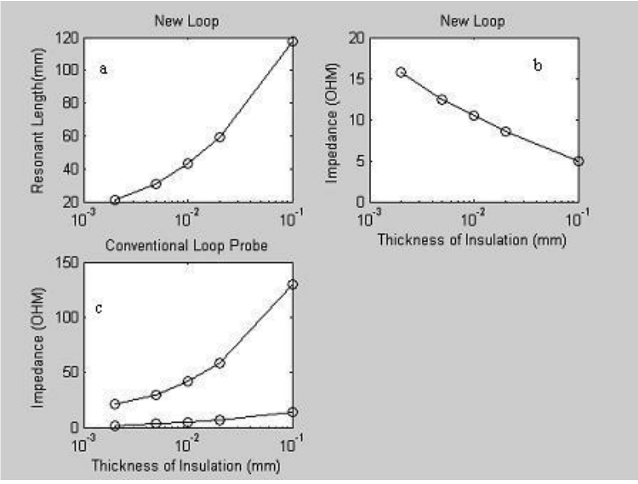

Fig. 2.a. Resonance length as a function of insulation thickness. Noth the small resonance length of the new probe.
Fig. 2.b. Real part of the new probe impedance as a function of insulation thickness. The imaginary part is zero. Note the decreasing of the impedance with insulation thickness.
Fig. 2.c. Real and imaginary parts of the conventional loop probe impedance as a function of insulation thickness. Note the small magnitude of the impedance real part relative to the imaginary part.

B. *SNR as a function of the insulation thickness*

Figures 3.a-c shows the intrinsic SNR distributions for three different insulation thicknesses of the new probe and the loop counterparts in the axial direction. They are for one un-insinuated, one with 0.01 mm insulation, and one with .1mm insulation. Each probe length is set to resonance length of new probe. These figures show the SNR increases for the new probe but decreases for the loop antennas by increasing the insulation thickness. In addition, uniformity of the SNR for the new probe in the axial direction is increased. The length of the axial simulation line is 60 mm in the z-axis; it is spaced 4 mm from the probe in the x-axis direction (see Fig. 1).

Figures 3.d-f show the intrinsic SNR distribution for three different insulation thicknesses of the new probe and the loop counterparts in the radial direction. They are one un-insinuated, one with 0.01 mm of insulation, and one with 0.1 mm of insulation. Each probe length is set to the resonance length of new probe. By increasing the insulation thickness from bare-case to 0.1 mm, the SNR peak increases upto 172% for the new probe and decreases 85% for the loop counterpart. By adding 0.01 mm of insulation, the ratio of the SNR peak for the new probe to the loop probe is 1.45. For the bare case, the slop of the SNR distribution for the new probe is better than the loop probe, but decreases 50% for 0.01 mm of insulation thickness. The length of the radial simulation is 20 mm and placed at 5-mm distance from the top of the probe (see Fig. 1).

In Figure 4, we have plotted the distribution of the SNR for the new probe in the bare case and 4 different thicknesses of insulation. These figures verify the results of the previous figures and clearly show that increasing the insulation thickness for the new probe in the given range increases the magnitude of the SNR.

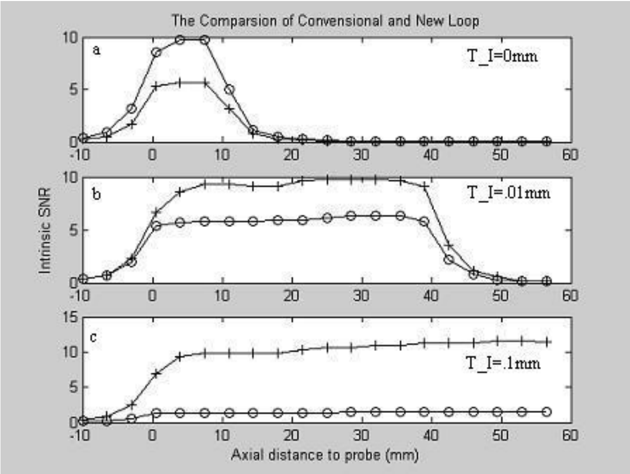

Fig. 3.a-c. Intrinsic SNR distribution along the axial direction with 3 insulation thicknesses for the new probe (+) and the conventional loop probe (o). Note the flatness of the SNR in the axial direction and the remarkable increase in the new probe SNR relative to the conventional counterpart.

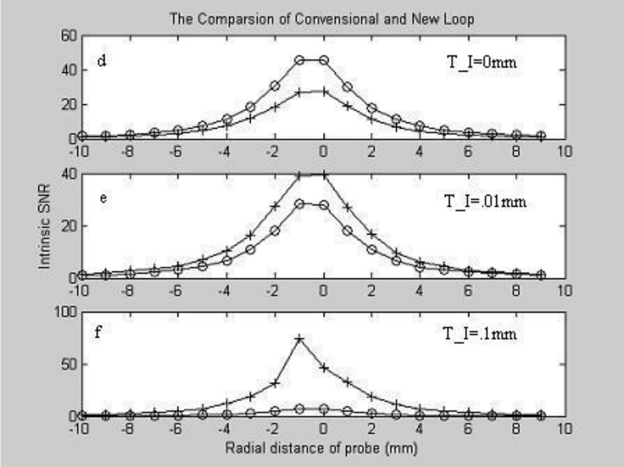

Fig. 3.d-f. Intrinsic SNR distribution along the radial direction with 3 insulation thicknesses for the new probe (+) and the conventional loop probe (o). T_I: Insulation Thickness. Note the high magnitude of the new probe SNR in T_I = 0.1 mm insulation.

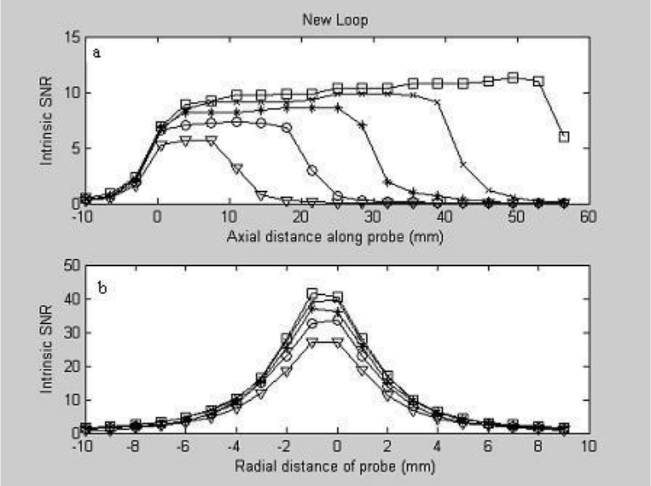

Fig. 4.a-b. Intrinsic SNR distribution along the axial and radial directions with the bare case (▽) and 4 insulation thicknesses: 0.002 (o); 0.005(+); 0.01(×); and 0.01(□) mm for the new probe. Note the increasing of the SNR and the axial fied of view for the new probe by increasing the insulation thickness.

V. DISCUSSION

A. Effect of insulation on the resonance length and real part of the input impedance

For the new probe, the insulation increases the resonant length and decreases the real part of the probes input impedance. In the human body, the quarter wavelength is about 10 cm; however, the resonance length of the new probe is only 1.1 cm in the bare case. For the traditional loop, with the same specifications as the new probe, the input impedance is 0.77+j13.8 OHM. Therefore, a matching circuit is necessary for the conventional small loop probes to maximize power transmission.

B. Effect of insulation on SNR distribution

Adding insulation to the probe has the effect of increasing the probe's SNR according to the intrinsic SNR formula. Note that by adding insulation and using resonance length, H_+ increases and R decreases.

Figures 3-4 show that the magnitude of the SNR distribution for the new probe is more than the loop probe in the radial and axial directions. In addition, the magnitudes of these quantities increase by increasing the insulation thickness. Increasing the SNR can produce high quality MR images while increasing of the SNR uniformity decreases motion and ghost artifacts of the MRI [7,8].

We should add that the higher performance of the new probe is a result of the gap and the two-folded design of the probe. Using these ideas increases the SNR of the probe in the insulated cases and shortens the resonance length of the probe.

VI. CONCLUSION

We analyzed a new dual-turn loop probe for its SNR, impedance, and uniformity inside a homogeneous material. We demonstrated that the new small intravascular probe increases the magnitude of the SNR significantly. The small size of the probe, in the bare and thin insulated cases, causes the probe to be optimal for imaging of the torso coronary arteries. Further research is required to evaluate this probe for various intravascular imaging applications.

REFERENCES

[1] E. Atalar, P.A. Bottomelly, O. Ocali, L. C. Correia, M.D. Keleman, J. A. Lima, and E. A. Zerhouni, “High resolution intravascular MRI and MRS by using a catheter receiver coil,” Magn. Reson. Med, vol. 36, pp. 595-605, 1996.

[2] H. H. Quick, M. E. Ladd, G. G. Zimmermann-Paul, P. Erhart, E. Huffman, J. F. Debatin, “Single loop coil concepts for intravascular MR imaging,” J. Magn. Reson. Imaging, vol. 9, pp. 751-758, 1999.

[3] A. J. Martin. A. I. Gottlieb, R. M. Henkelman, “High resolution MR imaging of human arteries,” J. Magn. Reson. Imaging, vol. 5, pp. 93-100, 1995.

[4] O. Ocali, E. Atalar, “Ultimate intrinsic SNR in MRI,” J. Magn. Reson. Med., vol. 39, pp. 462-473, 1998.

[5] H. Vessel, R. E. Collin, “The signal to noise Ratio of nuclear magnetic resonance surface coils and applications to a lossy dielectric cylinder model-part 1: theory,” IEEE. Trans. Biomed. Eng, vol. 42, pp. 497-506., 1995.

[6] D. A. Pozar, Microwave imaging. New Yourk: Wiley, 1990..

[7] A. J. Martin, R. M. Henkelman, “Intravascular MR imaging in a porcine animal Model,” J. Magn. Reson. Imaging, vol. 32, pp. 224-9, 1994.

[8] M. Mohammadzadeh, A. Tavakoli, M. Shahabadi, H. Soltanian-Zadeh, “Design and construction of a new intravascular probe with improved specifications for coroner vascular imaging by MRI,” in the Proc. of the 11th Iranian Conf. on Biomedical Engineering, ICBME 2004, pp. 11.